

The transition phase of the deviation vector of nearby orbits

This article has been downloaded from IOPscience. Please scroll down to see the full text article.

2001 J. Phys. A: Math. Gen. 34 1513

(<http://iopscience.iop.org/0305-4470/34/7/322>)

View [the table of contents for this issue](#), or go to the [journal homepage](#) for more

Download details:

IP Address: 171.66.16.101

The article was downloaded on 02/06/2010 at 09:50

Please note that [terms and conditions apply](#).

The transition phase of the deviation vector of nearby orbits

Ch L Vozikis

Department of Physics, Section of Astrophysics, Astronomy & Mechanics, Aristotles University of Thessaloniki, 54006 Thessaloniki, Greece

and

Department of Informatics and Communications, Technological Education Institute of Serres, 62100 Serres, Greece

Received 15 September 2000, in final form 4 January 2001

Abstract

Using a simple 2D area-preserving map we study the evolution of the deviation vector ξ of two initially nearby orbits. It is known that the deviation vector in each point is aligned along a preferable direction, which in the case of regular orbits is the direction of the tangent line to the invariant curve at that point, having also a specific value defined as the ‘stretching number’ at this point. Before the deviation vector takes its preferred direction and value it passes through a transient period. This transient period is found to be very short in the case of chaotic orbits while it is quite long for regular orbits. The initial orientation plays a minor role on the length of the transition phase except in the case when the initial ξ is almost perpendicular to the invariant curve. In this latter case the transition phase becomes quite extended. Analytic calculations suggest that as the iteration number n increases, in the case of chaotic orbits, the deviation vector tends to its preferred value exponentially, while it evolves with an n^{-1} power law in the case of regular orbits. Numerical results support the analytic predictions.

PACS numbers: 0545, 0540

1. Introduction

One of the most serious problems one encounters when dealing with non-integrable dynamical systems is to be able to distinguish (as early as possible) an ordered trajectory from a chaotic one.

Starting from the pioneering work of Hénon and Heiles (1964), a lot of methods, that reveal the chaotic or ordered nature of an orbit, have been developed. One of the most common tools is the calculation of the Lyapunov characteristic number (LCN) (Benettin *et al* 1976, Froeschlé 1984). The LCN method is based on the calculation of the divergence of two nearby orbits, or equivalently, of the evolution of the deviation vector ξ , which can be considered as the vector that connects at each time step the positions of the two nearby orbits.

Based on the same idea, i.e. the study of the deviation vector, other, more efficient, methods have been proposed. Froeschlé *et al* (1993) and Voglis and Contopoulos (1994) developed a method based on the probability density function of the ‘stretching numbers’, while Froeschlé *et al* (1997) proposed the use of the fast Lyapunov indicators (FLI). Voglis *et al* (1998, 1999), studying the properties of the probability density function analysis of the ‘stretching numbers’, proposed a very efficient method, namely the ‘dynamical spectral distance’ (DSD) method. Recently, Vozikis *et al* (2000) proposed a method based on the frequency analysis (power spectrum) of ‘stretching numbers’. This method is fast and efficient and can be applied to systems with any number of degrees of freedom.

Although the methods based on the deviation vector are widely used, so far its behaviour has not been studied in detail. There is one point in particular, the early time evolution of the deviation vector, which may significantly affect the results obtained from the methods mentioned above. Starting from a given orientation of ξ , the deviation vector evolves and after some time it orientates to some preferable direction, which is not only a characteristic of the model but also depends on the particular orbit. This early time evolution of the deviation vector is usually called ‘the transition phase’ or ‘the transient period’ of the deviation vector.

The aim of the present paper is to throw some light on this transient period, in order to have a better understanding of this phenomenon and the way it may affect the results of the methods that are based on the analysis of the evolution of the deviation vector.

In the majority of the problems in nonlinear dynamics an analytic approach is rather hard, if not impossible. An analytic method, mainly for ergodic systems, based on *evolution operators* was proposed and used by Cvitanović and Vattay (1993) and Pollner and Vattay (1996) (see also the web book ‘Classical and Quantum Chaos’ by Cvitanović *et al* (2000)). Their analytic approach gives very satisfactory results in calculating average quantities, as for example the Lyapunov exponents. Although our approach is mainly numerical, some analytic results will also be given.

The paper is organized as follows. The model and the method used for this study are presented in section 2, while section 3 deals with the problem of computational errors. Section 4 is devoted to the study of the orientation of the deviation vector and its dependence on various parameters. Section 5 presents some analytic results on the evolution of the deviation vector. Finally, section 6 presents a discussion on the conclusions of this paper.

2. The model and the method

One of the most frequently used test models in dynamics is the 2D standard map, which appears in the literature in many forms. One of them, in (θ, J) coordinates, is given by the following set of recursive equations/relations

$$\begin{aligned} J_{n+1} &= J_n + k \cos(\theta_n) && \text{mod } 2\pi \\ \theta_{n+1} &= \theta_n + J_{n+1} && \text{mod } 2\pi. \end{aligned} \quad (1)$$

The parameter k is usually called the ‘stochasticity parameter’. I consider here the cases $k = 0.7, 0.9$ and 1.2 , which are cases where the map possess both regular and chaotic regions.

Starting an orbit from a point (θ_0, J_0) we define the deviation vector ξ as the 2D vector distance of a second orbit $(\theta + \xi_\theta, J + \xi_J)$ that starts at an infinitesimal distance $\xi = \sqrt{\xi_\theta^2 + \xi_J^2}$ from the first one. The direction of the ξ vector can be given by the angle ϕ between ξ and the positive θ -axis.

The evolution of ξ can be traced using the *variational equations*,

$$\begin{aligned}\xi_{J_{n+1}} &= \xi_{J_n} - \xi_{\theta_n} k \sin \theta_n \\ \xi_{\theta_{n+1}} &= \xi_{\theta_n} + \xi_{J_{n+1}}.\end{aligned}\quad (2)$$

A quantity of special interest is the so-called ‘local LCN’ (Froeschlé *et al* 1993) or ‘stretching number’ (Voglis and Contopoulos 1994),

$$a_n = \ln \frac{\xi_n}{\xi_{n-1}}. \quad (3)$$

Almost all methods that are based on the analysis of the deviation vector use a_n or a quantity depending on a_n . The LCN is defined by

$$\text{LCN} = \lim_{N \rightarrow \infty} \frac{1}{N} \sum_{n=1}^N a_n. \quad (4)$$

As mentioned in the introduction, the deviation vector ξ not only depends on the model used but also on the orbit under consideration. Moreover, it depends on the particular point along the orbit. On each point, along the orbit, ξ orientates to a preferable direction, which in the case of regular orbits is tangential to the invariant curve. The stretching number a , which depends on the norm of ξ , also reaches a specific value, which is characteristic of this point and is independent of the initial ξ . In order for ξ to reach this preferable direction and value, a certain number of past iterations is needed. This phase of iterations is called the ‘transition phase’ or ‘transient period’.

In order to study the transient period, one must perform test runs with different numbers of iterations and compare the properties of the final deviation vectors of the different runs. Since we must compare deviation vectors on the same point, we have to make runs with different iteration numbers N that do not start from the same point (as usual) but, on the contrary, end on the point studied.

To accomplish this task we have to first go back N iterations using the ‘backward’ map of equation (1)

$$\begin{aligned}\theta_n &= \theta_{n+1} - J_{n+1} \quad \text{mod } 2\pi \\ J_n &= J_{n+1} - k \cos(\theta_n) \quad \text{mod } 2\pi\end{aligned}\quad (5)$$

where n counts from -1 down to $-N$. Starting now from iteration $-N$, i.e. with (θ_{-N}, J_{-N}) , and giving to ξ an initial value ξ_{init} we use the ‘forward’ map of (1) to calculate ξ_0 . Using this procedure with different values of N we always calculate the ξ_0 of the same point but with a different evolution history, which depends on N .

It should be noted that since all methods use the relative deviation ξ_{n+1}/ξ_n and since equations (2) are linear, only the initial orientation of ξ plays a role and not its norm. Therefore one may use any value for ξ_{init} .

3. Numerical errors

Before considering the actual analysis of the evolution of the deviation vector, there is a very sensitive point one has to deal with, i.e. the numerical errors which are introduced in the computations.

When one, calculating an orbit, starts from a given position, goes back N iterations and then iterates forward, it is possible (actually it is absolutely certain) that one will not return to the same point from which one started. This is mainly due to numerical round-off errors which are cumulatively added from one iteration to the next.

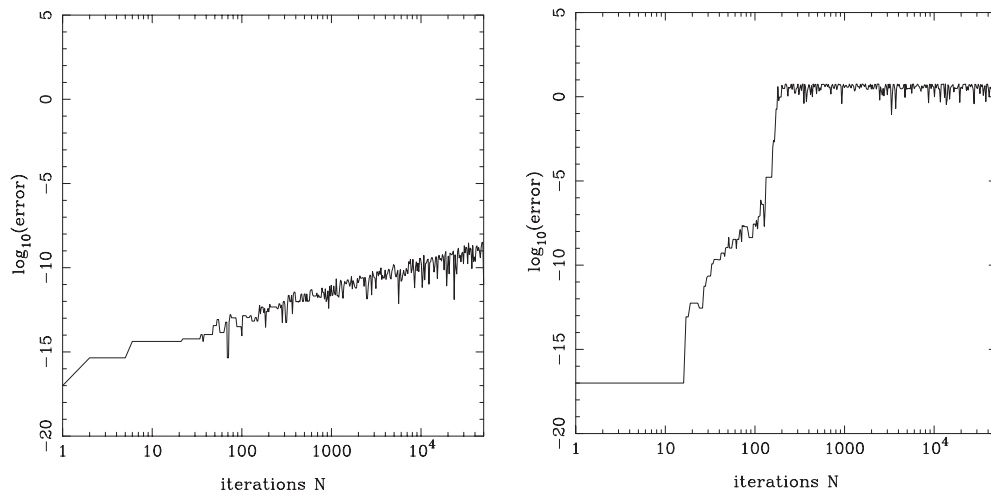


Figure 1. The error of the backward–forward procedure as a function of total iteration number N for a regular orbit (left) starting at $(\theta, J) = (0.5, 0.8)$ and a chaotic orbit (right) starting at $(0.5, 0.5)$, when $k = 0.7$.

Assuming that the properties of the deviation vector change smoothly from point to point in the phase space (with the exception perhaps of narrow boundaries between chaotic and regular regions), then we accept our results only if after going back and forth we end at a point which lies very near to the one where we started. Therefore, to check the validity of our results we define the error of the backward and forward procedure as the 2D distance between the initial and the final position. Of course the maximum possible error for the standard map is $2\pi\sqrt{2}$, i.e. starting from $(0, 0)$, going back and returning to $(2\pi, 2\pi)$!

The left frame of figure 1 shows the evolution of the error as a function of iteration number N for a regular orbit that starts from $(\theta, J) = (0.5, 0.8)$ when $k = 0.7$. As we can see the error remains small even for large values of N . It is around 10^{-8} for $N = 5 \times 10^4$. In contrast, for a chaotic orbit with initial position $(0.5, 0.5)$, as we can see on the right frame of figure 1, the error grows exponentially and after only 150 iterations it reaches its maximum value. Other orbits also present similar results. Thus, if an orbit is regular we can follow the evolution of the deviation vector going backwards using a large number of iterations. When dealing with chaotic orbits we have to be careful not to exceed 150 iterations. This seems to be a problem but as we will see in the next section, in the chaotic case, the necessary iterations for the deviation vector to find its preferable value are less than 150. The fast growth of the error is an indication of the stochasticity of the orbit and shows how fast it ‘loses its memory’.

4. The evolution of the deviation vector

When analysing the evolution of the deviation vector ξ one needs to check the evolution of the ‘stretching number’, a_N , defined by equation (3), which shows the relative change of the norm of vector ξ and the evolution of the orientation of ξ , which can be expressed by the angle ϕ between the ξ and the positive θ -axis.

Starting with a regular orbit, for $k = 0.7$, with initial position at $(\theta, J) = (0.5, 0.2)$ and with initial deviation vector ξ at the direction $(\xi_\theta, \xi_J) = (1, 1)$, we plot in the left frame of figure 2 the different values of the stretching number a as a function of the iteration number N .

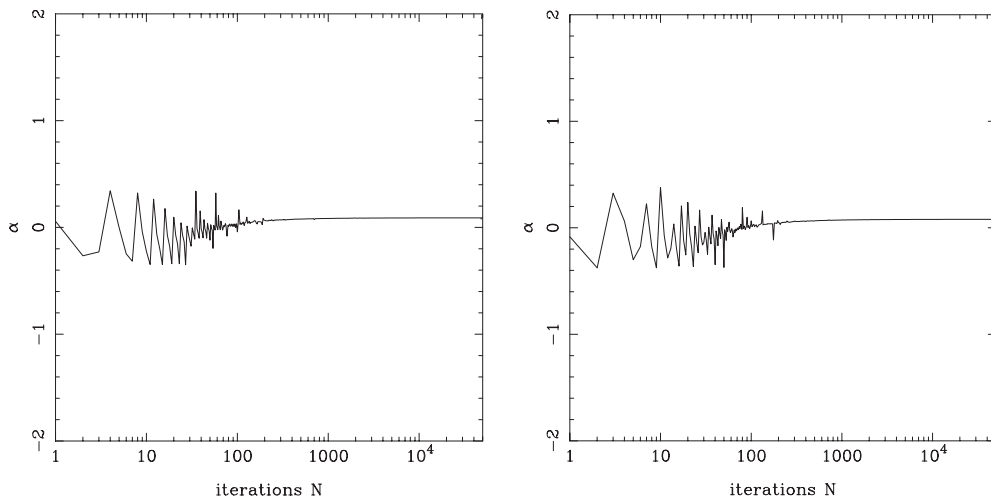


Figure 2. The dependence of the stretching number a on the iteration number N of their ‘past history’, for two regular orbits. Initial conditions are $(\theta, J) = (0.5, 0.2)$ and the stochasticity parameter k : left frame $k = 0.7$, right frame $k = 0.9$.

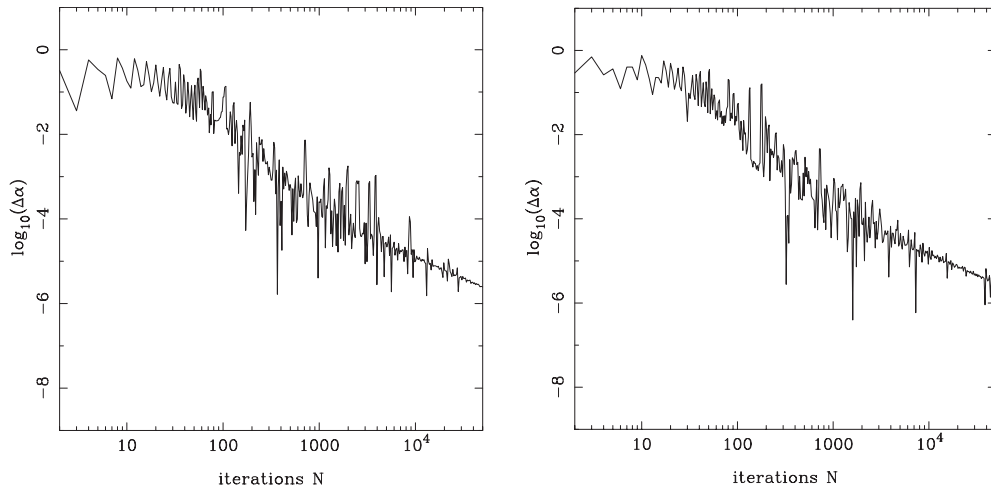


Figure 3. The dependence of relative change Δa of the stretching number on the iteration number N , for the two regular orbits of figure 2. Initial conditions are $(\theta, J) = (0.5, 0.2)$ and the stochasticity parameter k : left frame $k = 0.7$, right frame $k = 0.9$.

We see that for small values of N , a takes quite different values. As N increases, a seems to oscillate and tends to a specific value. Similar results are obtained for any other regular orbit tested. The right frame of figure 2 shows the dependence of a from N for an other regular orbit starting from the same (θ, J) position but for $k = 0.9$.

To see how fast a saturates to its preferred value, it is much better to plot its relative change Δa as N increases. Defining Δa as:

$$\Delta a = a_{N+1} - a_N \tag{6}$$

we plot in figure 3 the change of Δa as N increases for the two regular orbits of figure 2. As expected, Δa drops as N increases showing the trend of ξ to find its preferred value. An

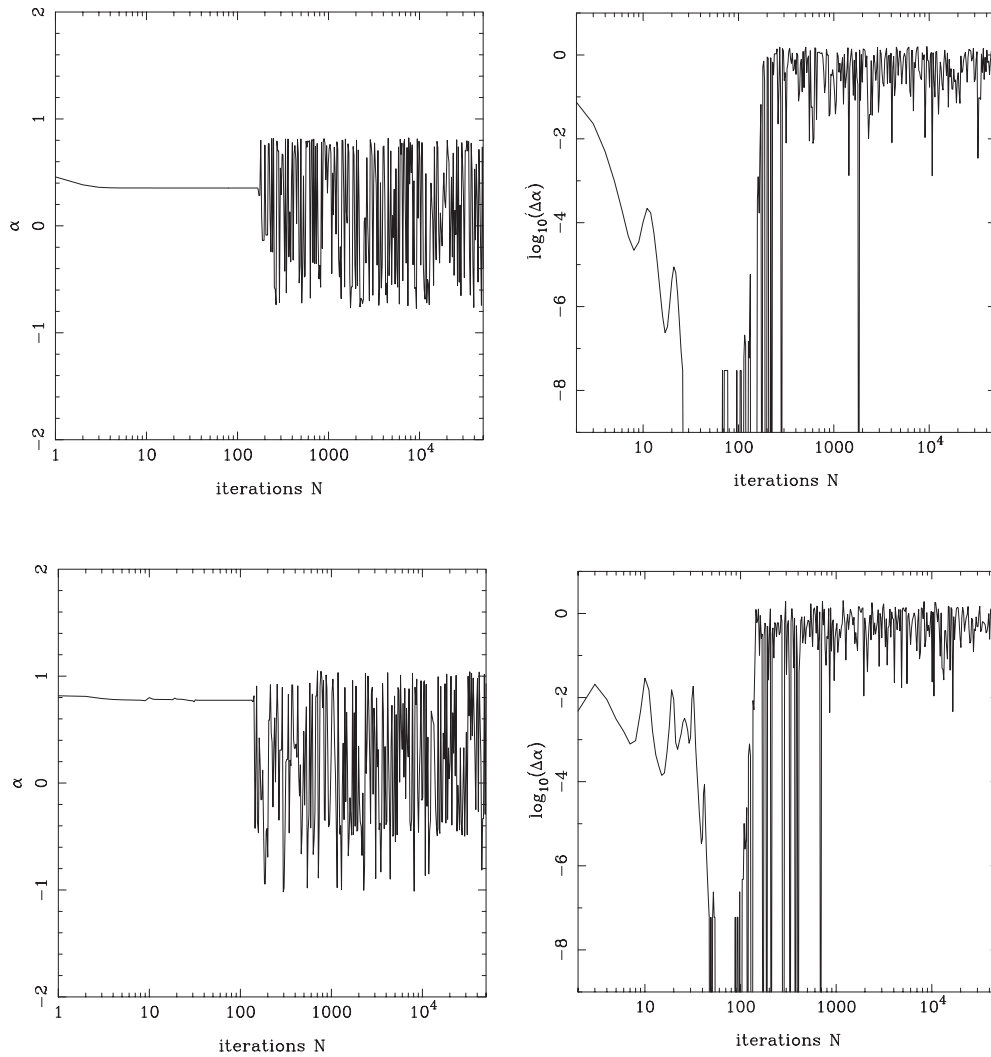


Figure 4. The dependence of a (left frames) and Δa (right frames) on the iteration number N , for two chaotic orbits. The upper row is for an orbit starting at $(\theta, J) = (0.5, 0.5)$ when $k = 0.7$, while the orbit in the lower row starts at $(\theta, J) = (0.1, 0.9)$ with $k = 1.2$. The range of iteration number N in the lower row is truncated to the point where the error becomes significant.

interesting point that figure 3 shows is the almost linear dependence of Δa on $1/N$.

On the other hand, chaotic orbits present a faster saturation. Figure 4 shows a and Δa (left and right frames, respectively) for two chaotic orbits, one starting at $(\theta, J) = (0.5, 0.5)$ when $k = 0.7$ (upper row) and one at $(\theta, J) = (0.1, 0.9)$ when $k = 1.2$ (lower row). As we can see from the left parts of both frames, a needs less than 30 iterations to find its preferred value. The phase with wide oscillations, in the right part of both frames, is not due to a real change of the value of a but is due to numerical errors, as also shown in figure 1. Going back to figure 1 we see that for $N > 150$ our ‘backward and forward’ procedure fails. The a we record here for high values of N is for a point in phase space far away from the one where we started and wanted to study, i.e. $(\theta, J) = (0.5, 0.5)$. Thus, it is normal for the a to be quite

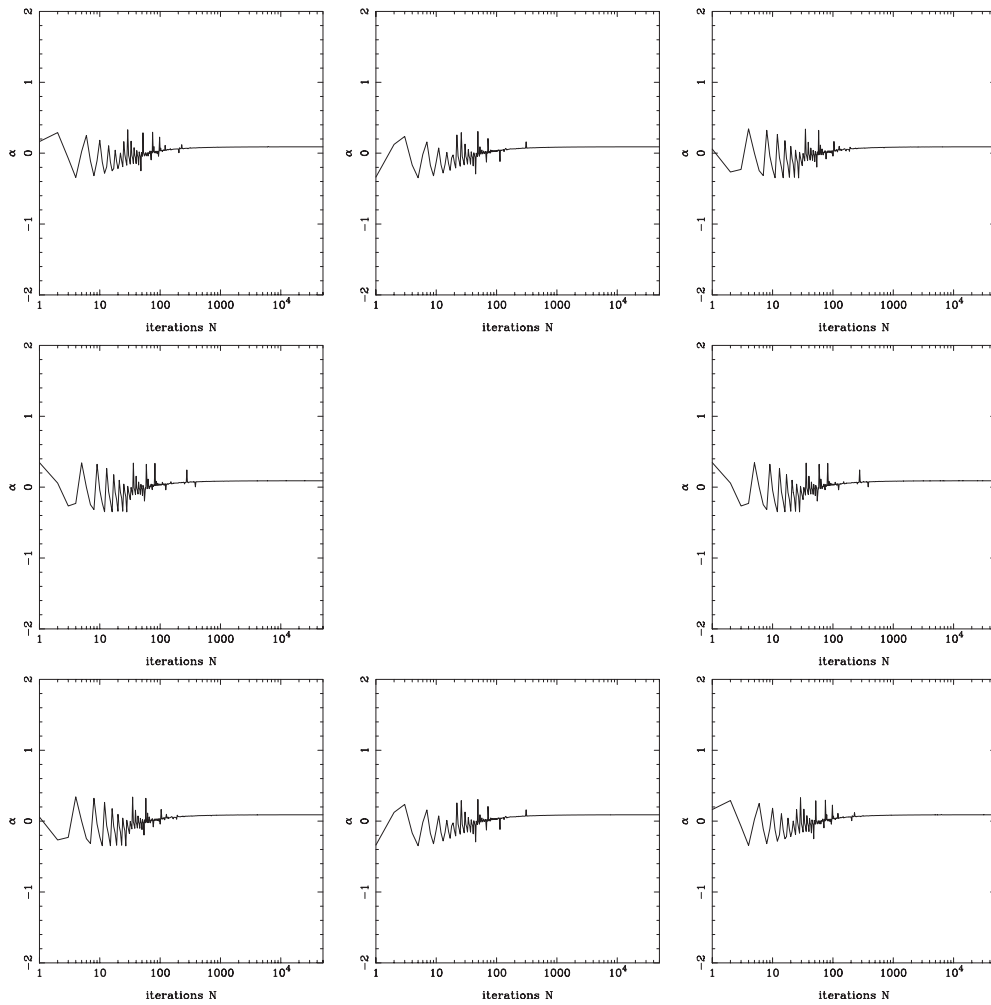


Figure 5. Stretching number a as a function of the number of past iterations N for a regular orbit with $(\theta_0, J_0) = (0.5, 0.2)$ and $k = 0.7$ but with different initial ξ . The initial deviation vectors (ξ_θ, ξ_J) are: top $(-1, 1), (0, 1), (1, 1)$; middle $(-1, 0), (1, 0)$; and bottom $(-1, -1), (0, -1), (1, -1)$.

different from the one of the point under consideration. So one should neglect any results with $N > 120$ where the error is higher than 10^{-5} .

It would be interesting to see whether this transition phase depends on the choice of the initial direction of the deviation vector. Figure 5 shows the transition phase of a for the regular orbit with $(\theta, J) = (0.5, 0.2)$ and $k = 0.7$ using eight different directions for the initial ξ , i.e. from the top to bottom row and from the left to right frame $(-1, 1), (0, 1), (1, 1), (-1, 0), (0, 1), (-1, -1), (0, -1)$ and $(1, -1)$. As we can see, the transition phase is different but in all cases the preferred value of a is reached after a few hundred iterations. One point that we can observe is that there is a ‘point’ symmetry in the figures. The pattern of the transition phase of a with initial deviation vector (ξ_θ, ξ_J) and that with $(-\xi_\theta, -\xi_J)$ are the same. Of course this is an intrinsic property of the variational equations (2). Equation (2) are linear with respect to (ξ_θ, ξ_J) ; thus if $\xi_n = (\xi_{\theta_n}, \xi_{J_n})$ resolves to $\xi_{n+1} = (\xi_{\theta_{n+1}}, \xi_{J_{n+1}})$, then $-\xi_n = (-\xi_{\theta_n}, -\xi_{J_n})$

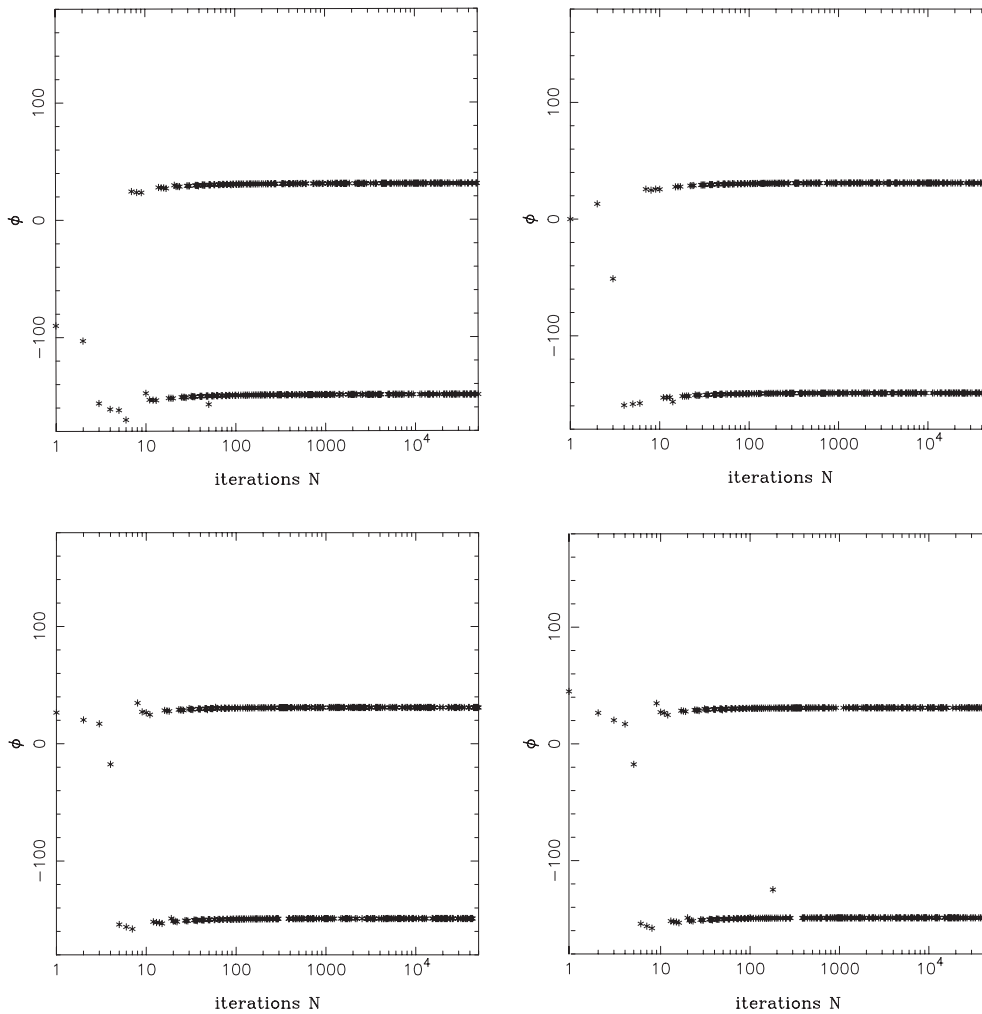


Figure 6. The orientation angle ϕ of the deviation vector ξ as a function of the number of past iterations N for a regular orbit with $(\theta_0, J_0) = (0.5, 0.5)$ and $k = 1.2$ but with four different initial ξ . In the first row the initial deviation vectors are $(\xi_\theta, \xi_J) = (-1, 1), (0, 1)$ and in the second $(1, 1), (1, 0)$.

will resolve to $-\xi_{n+1} = (-\xi_{\theta_{n+1}}, -\xi_{J_{n+1}})$. Since a depends only on the norm of ξ , a will be the same in both cases.

The next step is to examine the evolution of the direction of the deviation vector ξ . Figures 6 and 7 present the change of the angle ϕ between the vector ξ and the positive θ -axis. Figure 6 is for the regular orbit with $(\theta, J) = (0.5, 0.5)$ while figure 7 is for a chaotic orbit with $(\theta, J) = (0.1, 0.9)$. In both cases the stochasticity parameter is taken to be equal to $k = 1.2$. For each orbit the four frames correspond to four different initial orientations of ξ ; namely, from left to right, top row $(-1, 1), (0, 1)$ and bottom row $(1, 1), (1, 0)$. As we can see, after a small transient period the deviation vector is finally aligned along a line but its preferred direction may differ by 180° . Which of the two orientations ξ will take depends on the number of past iterations N and the initial orientation of ξ with respect to the invariant curve. Once

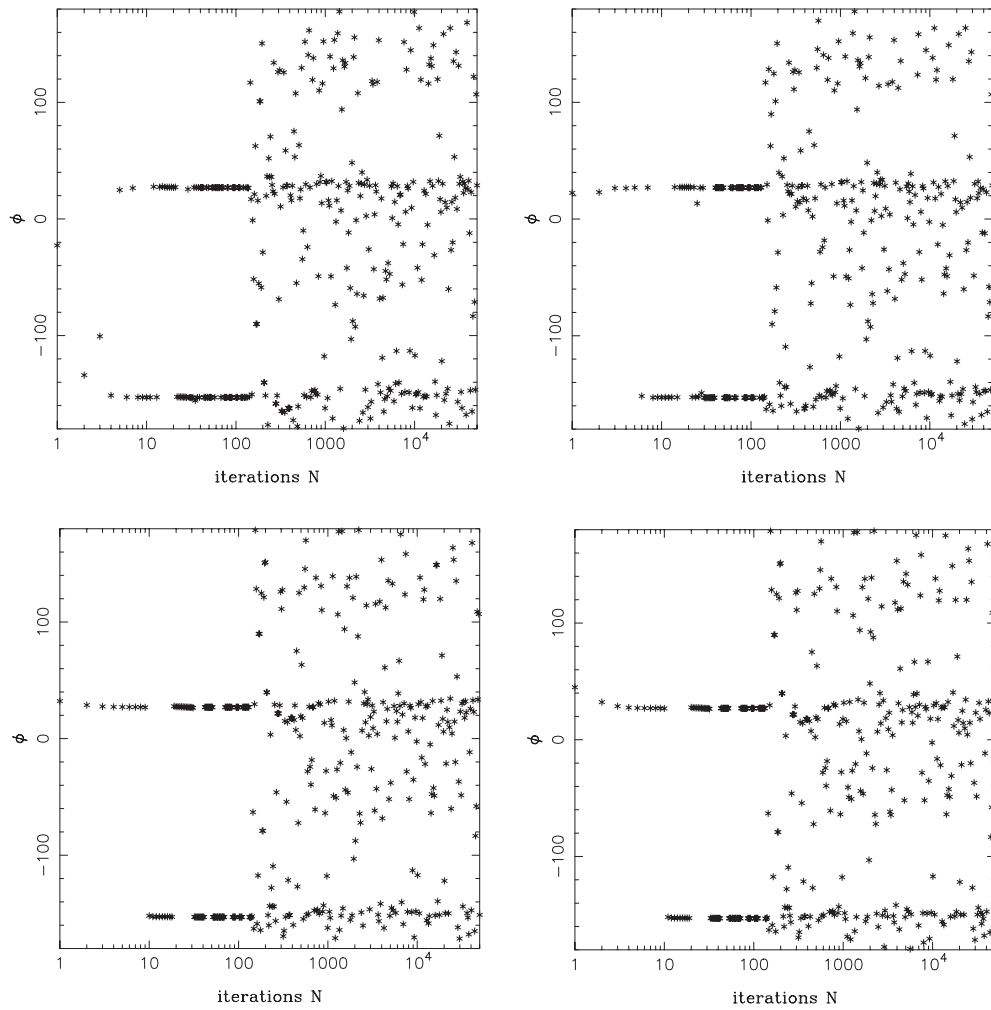


Figure 7. Same as figure 6 but for a chaotic orbit with $(\theta_0, J_0) = (0.5, 0.5)$ and $k = 1.2$. In the first row the initial deviation vectors are $(\xi_\theta, \xi_J) = (-1, 1), (0, 1)$ and in the second $(1, 1), (1, 0)$.

again, we remind the reader that the irregular pattern for $N > 100$ of the chaotic orbit is due to numerical errors. The preferred line of alignment of the deviation vector is independent of the initial direction of ξ . This is better illustrated in figure 8 where we have plotted the value of the final ϕ as a function of the initial ϕ for the regular orbit of figure 6 using $N = 10$ (upper left), 40 (upper right), 100 (lower left) and 400 (lower right). The analysis of the plots in the initial ϕ is 0.1° . As we can see, there is a range of initial ϕ which is 180° wide and leads to one orientation of ξ and another range of initial ϕ which leads to the opposite orientation. The change from one orientation to the other is quite sharp, especially for high values of N . The exact value of the initial ϕ where we have this change from one orientation to the other is the angle for which the initial ξ is perpendicular to the invariant curve.

Combining figure 8 with 9, which is the same as figure 8 but now the value of a instead of ϕ is plotted, we can see that only a few iterations are sufficient for ξ to reach its preferred value and direction. This holds true for almost all values of initial ϕ . Nevertheless, there are

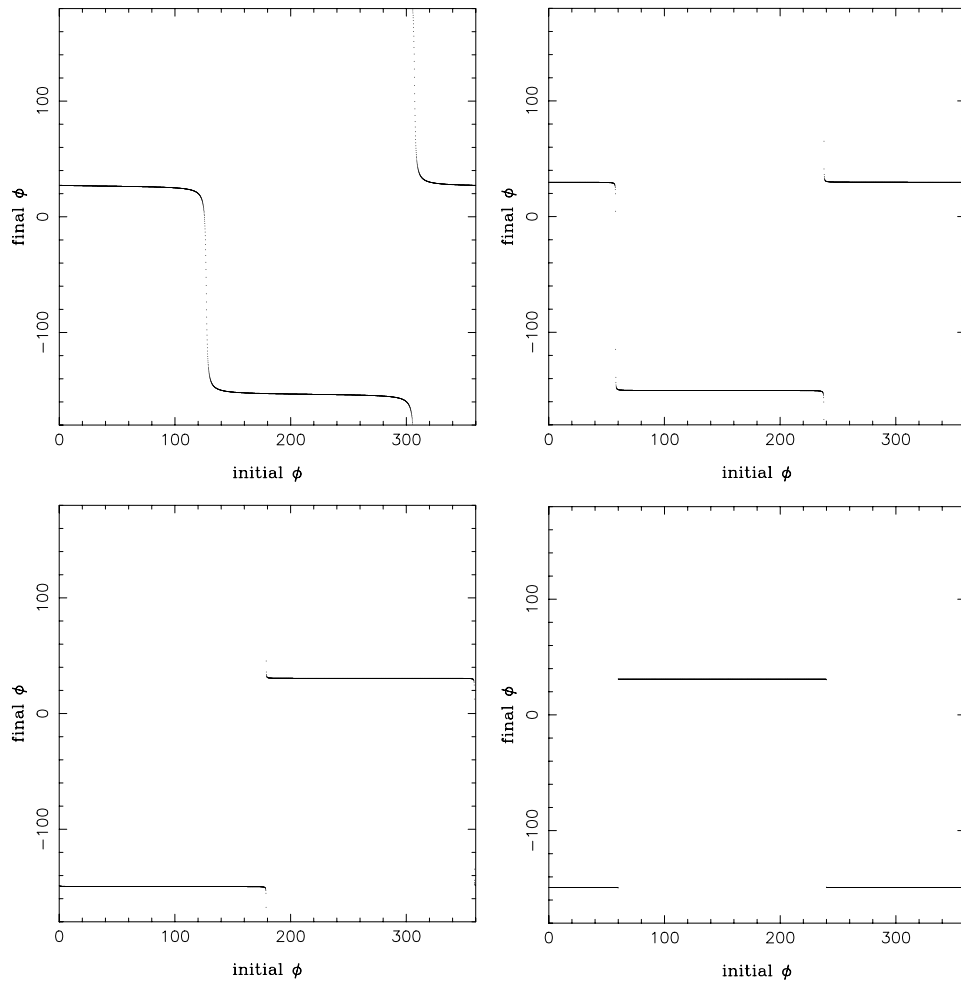


Figure 8. The final orientation angle ϕ of the regular orbit of figure 6 as a function of the initial ϕ . The number of past iterations are $N = 10, 40, 100$ and 400 . In the first row the initial deviation vectors are $(\xi_\theta, \xi_J) = (-1, 1), (0, 1)$ and in the second $(1, 1), (1, 0)$.

two small sets of values of initial ϕ where a fails to converge as fast. These two sets are at the neighbourhood of the turning points where the final ϕ changes its value by 180° . As we can see, the sharper the change of ϕ is, the better the convergence of a will be. The same results also hold true for chaotic orbits, but in this case the convergence is much faster and with only 40 iterations there is no value of initial ϕ which resolves to an observably different value of a .

5. Analytic approach

First, let us rewrite the variational equations (2) in a matrix form.

$$\begin{pmatrix} \xi_J \\ \xi_\theta \end{pmatrix}_{n+1} = \begin{pmatrix} 1 & -k \sin(\theta_n) \\ 1 & 1 - k \sin(\theta_n) \end{pmatrix} \begin{pmatrix} \xi_J \\ \xi_\theta \end{pmatrix}_n \quad (7)$$

or

$$\xi_{n+1} = A \cdot \xi_n. \quad (8)$$

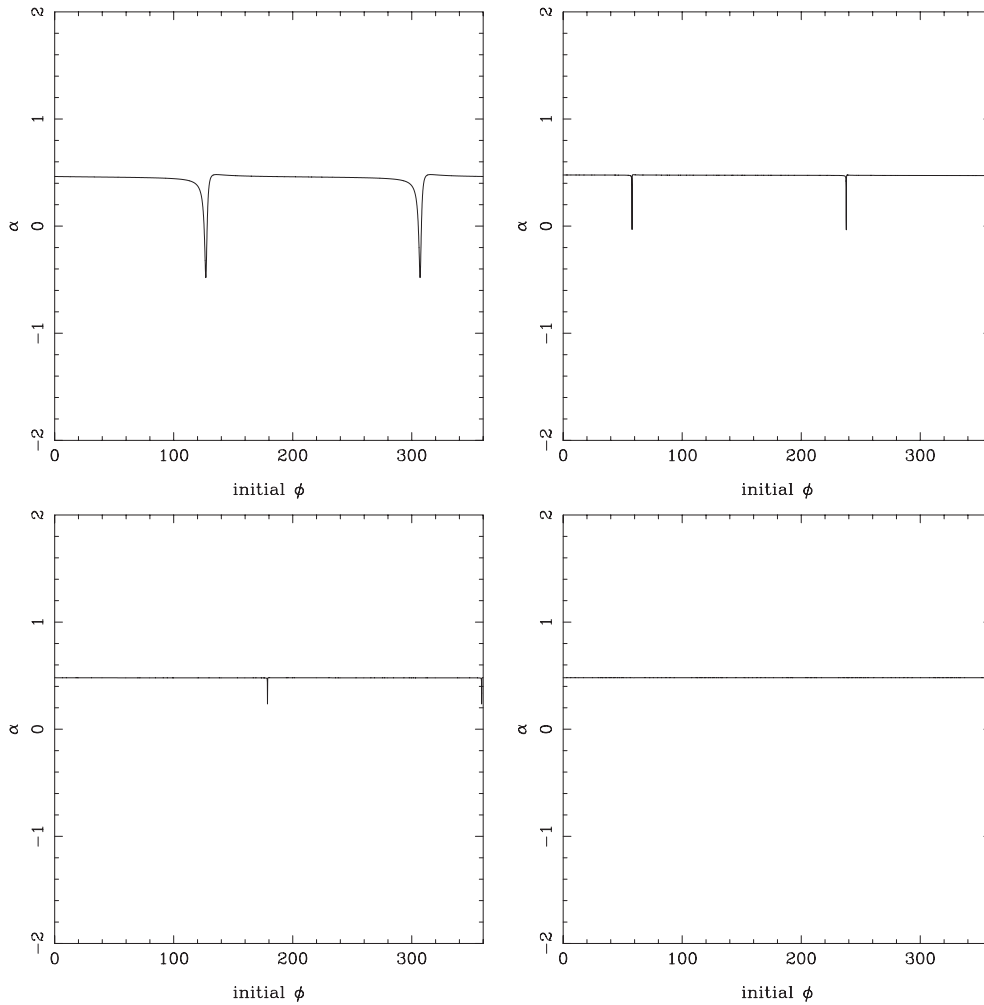


Figure 9. Same as figure 8 but with the value of the final stretching number a plotted instead of the final ϕ . In the first row the initial deviation vectors are $(\xi_\theta, \xi_J) = (-1, 1), (0, 1)$ and in the second $(1, 1), (1, 0)$.

Setting $-k \sin(\theta_n) = q$ the eigenvalues of matrix A are

$$\lambda_1 = \frac{1}{2} \left(2 + q + \sqrt{4q + q^2} \right) \quad \lambda_2 = \frac{1}{2} \left(2 + q - \sqrt{4q + q^2} \right) \quad (9)$$

with

$$\lambda_1 \lambda_2 = 1. \quad (10)$$

For a given positive value of k , q takes values in the interval $[-k, 0)$ when $\theta \in (0, \pi)$, while, when $\theta \in [\pi, 2\pi]$, q takes values in the interval $[0, k]$. Thus, when $\theta \in [\pi, 2\pi]$ the eigenvalues of matrix A are real numbers, with $\lambda_1 \geq 1$ as the leading eigenvalue and $\lambda_2 = \lambda_1^{-1}$. When q is negative the two eigenvalues are complex conjugate numbers (i.e. $\lambda_2 = \lambda_1^*$) on the unit circle.

The mapping, for $k \neq 0$, has a period 1 hyperbolic (unstable) fixed point at $J = 0, \theta = 3\pi/2$, and for $k \in (0, 4)$ an elliptic (stable) fixed point at $J = 0, \theta = \pi/2$. For the values

of k used, a wide region around the hyperbolic point is chaotic.

Let us take a point (θ_n, J_n) near the hyperbolic point (the point belongs to a chaotic orbit) and an initial deviation vector ξ_n of unit length at this point. Matrix A has two real eigenvalues λ and λ^{-1} and two real eigenvectors v_1 and v_2 . The eigenvectors form a (non-orthogonal) base (except for the case $\lambda = 1$ where the two eigenvectors coincide) and any vector ξ can be written as a linear combination of v_1 and v_2

$$\xi_n = c_1 v_1 + c_2 v_2. \quad (11)$$

The angle φ of vector ξ from the ‘leading’ eigenvector v_1 can be characterized by the ratio c_2/c_1 . We will refer to this ratio as the ‘tangent’, in the base $v_1 v_2$, of the angle φ (although it is not the real $\tan \varphi$ since the base v_1, v_2 is not, in general, orthogonal).

$$\tan \varphi_n = \frac{c_2}{c_1}. \quad (12)$$

The effect of matrix A on the vector ξ_n is to expand it in the direction of v_1 and to contract it in the direction of v_2 . This results, in addition to the change of the norm of ξ , to a change in the direction of the vector. Matrix A tries to align ξ with the vector v_1 . The new vector ξ_{n+1} will now be

$$\xi_{n+1} = \lambda c_1 v_1 + \lambda^{-1} c_2 v_2 \quad (13)$$

and the tangent of the new angle is

$$\tan \varphi_{n+1} = \frac{\lambda^{-1} c_2}{\lambda c_1} = \frac{1}{\lambda^2} \tan \varphi_n. \quad (14)$$

Thus, since $\lambda > 1$, in each iteration the angle becomes smaller.

As we see from equation (3), the stretching number a at iteration n depends on the ratio of the norm of ξ at iterations n and $n - 1$. So, as already stated, we can renormalize ξ before the next iteration to be a unit vector. This way, the effect of the operation of matrix A in the previous $n - 1$ iterations is only a change to its orientation.

In each iteration, i , the orbit is at a different position, (θ_i, J_i) , and the matrix A_i has different eigenvectors and eigenvalues. Nevertheless, the leading eigenvector v_1 points, more or less, to the same direction, as can be seen in the left frame of figure 10 which shows the direction of eigenvector v_1 (in degrees) as a function of θ (in units of π). The lower curve is for $k = 0.7$, while the upper curve is for $k = 1.2$. Thus, after each iteration vector ξ is better aligned with the eigenvector of the next iteration.

From the above we can conclude that a converges to a specific value and Δa changes as

$$\Delta a \propto \frac{1}{\Lambda^{2N}} \quad (15)$$

where Λ can be considered to be a ‘mean’ eigenvalue.

In the right frames of figure 4, where the evolution of Δa is presented as a function of iteration number n for two chaotic orbits, we can see that, although Δa presents some oscillations its mean value follows the exponential law of equation (15). A linear least-squares fit of $N, \log_{10} \Delta a$, for the upper orbit of figure 4, gives a good agreement with equation (15) and a mean eigenvalue Λ of about 1.28 ± 0.02 .

For the regular orbits we will use a different approach. An invariant curve near the elliptic (stable) fixed point can be represented by elliptic motion around the fixed point, which with proper coordinate transformation can be reduced to circular motion (for a detailed analysis see the book ‘Regular and Stochastic Motion’ by Lichtenberg and Lieberman (1983)). A regular orbit is, in general, a quasi-periodic orbit, i.e. its rotational frequency is an irrational number.

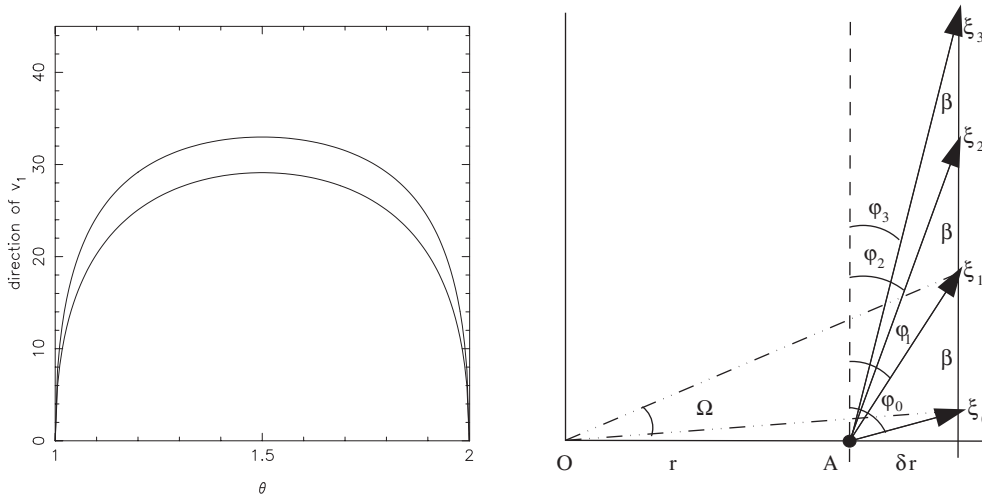


Figure 10. Left: the orientation angle of the eigenvector v_1 (in degrees) as a function of θ (in units of π). The upper curve is for $k = 1.2$ and the lower curve is for $k = 0.7$. Right: schematic analysis of the evolution of the deviation vector for the case of quasi-periodic orbits.

Let us take a quasi-periodic orbit with period m , i.e. which returns to approximately the same point after m iterations of the mapping. If we use a rotating frame of reference, which rotates with the same frequency as the orbit, then, after m iterations, the orbit will return to the same point. An initial deviation vector ξ_0 points to a point on another, nearby, quasi-periodic orbit, which has a slightly different rotational frequency. After m iterations this point will map to another point at a distance β from the first one (see the right frame of figure 10) and the deviation vector will become ξ_1 . If we denote by φ_0 the initial angle of ξ_0 from the tangent line of the invariant curve at the point studied, then successive steps will change the deviation vector and the angle φ to (ξ_1, φ_1) , (ξ_2, φ_2) and so on.

Since ξ is infinitesimally small, the invariant curve of the nearby quasi-periodic orbit can be considered, in the vicinity of the point studied, as a straight line. In addition, the distance β of successive points can be considered as a constant, which depends on the distance δr of the two orbits, the initial condition of the orbit under study (i.e. the point A) and of course the parameters of the model (in our case the parameter k)

As can be seen in figure 10, in each iteration the angle φ becomes smaller and smaller and the deviation vector ξ tends to the tangential direction. After n steps the angle φ will be

$$\tan \varphi_n = \frac{\xi_0 \sin \varphi_0}{\xi_0 \cos \varphi_0 + n\beta}. \tag{16}$$

The value of β depends on the distance r from the elliptic stable fixed point (which is the centre of the rotating coordinate system, point O in figure 10) and on the angle Ω , which depends on the difference of the rotation frequencies of the two nearby orbits. In the linear approximation

$$\Omega = c \delta r \tag{17}$$

where c is a constant depending on the point A and the model itself, and

$$\beta = r \sin \Omega = r\Omega = rc \delta r = C\delta r. \tag{18}$$

Since $\delta r = \xi_0 \sin \varphi_0$

$$\beta = C\xi_0 \sin \varphi_0 \tag{19}$$

and equation (16) becomes

$$\tan \varphi_n = \frac{\sin \varphi_0}{\cos \varphi_0 + nC \sin \varphi_0}. \quad (20)$$

As we can see from equation (20), the angle $\varphi \rightarrow 0$ as the iteration number $n \rightarrow \infty$. It is important to note that the evolution of the angle φ is independent from the norm of the initial deviation vector ξ and depends on the initial direction of ξ (angle φ_0) and of course on the particular orbit and model (parameter C). For large values of n the deviation vector ξ tends to its preferred tangential direction as n^{-1} , a result already observed numerically in figure 3.

Figure 10 (right) can also help us to calculate the ratio of the norms of two successive deviation vectors ξ_{j-1} , ξ_j .

$$\begin{aligned} \frac{\|\xi_j\|}{\|\xi_{j-1}\|} &= \frac{\xi_j}{\xi_{j-1}} = \frac{\sqrt{\xi_0^2 \sin^2 \varphi_0 + (\xi_0 \cos \varphi_0 + j\xi_0 C \sin \varphi_0)^2}}{\sqrt{\xi_0^2 \sin^2 \varphi_0 + (\xi_0 \cos \varphi_0 + (j-1)\xi_0 C \sin \varphi_0)^2}} \\ &= \sqrt{\frac{1 + j^2 C^2 \sin^2 \varphi_0 + jC \sin 2\varphi_0}{1 + (j-1)^2 C^2 \sin^2 \varphi_0 + (j-1)C \sin 2\varphi_0}}. \end{aligned} \quad (21)$$

As j becomes bigger

$$\frac{\xi_j}{\xi_{j-1}} = \frac{j}{j-1} \rightarrow 1. \quad (22)$$

It should be noted that ξ_{j-1} , ξ_j are not the deviation vectors of successive iterations of the map, but of successive steps of m iterations, since the quasi-periodic orbit returns to the same after m iterations. Therefore

$$\frac{\xi_j}{\xi_{j-1}} = \frac{\xi_{n+m}}{\xi_n} = \frac{\xi_{n+1}}{\xi_n} \frac{\xi_{n+2}}{\xi_{n+1}} \dots \frac{\xi_{n+m}}{\xi_{n+m-1}} = \prod_{j=1}^m \frac{\xi_{n+j}}{\xi_{n+j-1}}. \quad (23)$$

Since

$$\prod_{j=1}^m \frac{\xi_{n+j}}{\xi_{n+j-1}} \rightarrow 1 \quad (24)$$

as n becomes bigger,

$$\ln \left(\prod_{j=1}^m \frac{\xi_{n+j}}{\xi_{n+j-1}} \right) \rightarrow 0 \quad (25)$$

but

$$\begin{aligned} \ln \left(\prod_{j=1}^m \frac{\xi_{n+j}}{\xi_{n+j-1}} \right) &= \ln \frac{\xi_{n+1}}{\xi_n} + \ln \frac{\xi_{n+2}}{\xi_{n+1}} + \dots + \ln \frac{\xi_{n+m}}{\xi_{n+m-1}} \\ &= a_{n+1} + a_{n+2} + \dots + a_{n+m} = \sum_{j=1}^m a_{n+j}. \end{aligned} \quad (26)$$

Thus the sum of m successive stretching numbers tends to zero, as n increases, although individual stretching numbers may not. This directs us to the already well-known property of regular motion that the time (iteration) average of stretching numbers, i.e. the LCN, tends to zero.

6. Conclusions

In this paper we tried to throw some light on the transient period of the deviation vector of two nearby orbits using a simple 2D map.

It was already known that, for regular orbits, the deviation vector, after some time, is aligned along the tangent of the invariant curve. Nevertheless, even for chaotic orbits there is a preferable direction that the deviation vector tends to.

The transient period, before the deviation vector takes its preferred value and direction, is quite different for chaotic and for regular orbits. Chaotic orbits have a very short transient period. For the model tested, only 30–40 iterations are sufficient for the relative difference, Δa , of the stretching number to drop below 10^{-5} , as can be seen in figure 4 where Δa drops exponentially with increasing iteration number N . On the other hand, regular orbits seem to have a much longer transient period. In order to have the same (10^{-5}) value for Δa , one needs about 10 000 iterations. In regular orbits, Δa seems to drop almost linearly with $1/N$. Analytic predictions agree very well with the numerical results.

The transient period is found to depend very little on the initial orientation of the deviation vector. Nevertheless, if ξ is initially almost perpendicular to the invariant curve, the transient period becomes quite extended. For the exact perpendicular orientation of ξ the transient period may be extremely long.

Although we have restricted our study to a 2D mapping, similar results are also expected for Hamiltonian systems with two or more degrees of freedom. However Hamiltonian systems are not so simple. Mappings are simple recursive formulas, therefore ξ and a are calculated at specific (discrete) time steps, i.e. one iteration. In contrast, Hamiltonian systems may be characterized as ‘flows’. Thus the time step after which a is calculated and ξ is renormalized is ‘user defined’. It is possible that this renormalization time step affects the transient period and consequently the results of the chaos detecting methods. Therefore a more detailed investigation on the dependence of the evolution of ξ on the various parameters in Hamiltonian systems is needed and this will be addressed in a future paper.

Acknowledgments

I would like to thank the anonymous referee for drawing my attention to the analytic approach of the problem. Special thanks go to K Tsiganis for many fruitful discussions.

References

- Benettin G, Galgani L and Strelcyn J M 1976 *Phys. Rev. A* **14** 2338
 Cvitanović P and Vattay G 1993 *Phys. Rev. Lett.* **71** 4138
 Cvitanović P, Artuso R, Mainieri R and Vattay G 2000 *Classical and Quantum Chaos* (Copenhagen: Niels Bohr Institute) webpage <http://www.nbi.dk/ChaosBook/>
 Hénon M and Heiles C 1964 *Astron. J.* **69** 73
 Froeschlé C 1984 *Celest. Mech.* **34** 95
 Froeschlé C, Froeschlé Ch and Lohinger E 1993 *Celest. Mech. Dyn. Astron.* **51** 135
 Froeschlé C, Lega E and Gonzi R 1997 *Celest. Mech. Dyn. Astron.* **67** 41
 Lichtenberg A J and Leiberman M A 1983 *Regular and Stochastic Motion* (New York: Springer) p 183
 Pollner P and Vattay G 1996 *Phys. Rev. Lett.* **76** 4155
 Voglis N and Contopoulos G 1994 *J. Phys. A: Math. Gen.* **27** 4899
 Voglis N, Contopoulos G and Efthymiopoulos C 1998 *Phys. Rev. E* **57** 372
 ——— 1999 *Celest. Mech. Dyn. Astron.* **73** 211
 Vozikis Ch L, Varvoglis H and Tsiganis K 2000 *Astron. Astrophys.* **359** 386